Electron-Spin-Resonance Experiments on Antimony-Doped Germanium*

RICHARD E. PONTINEN† AND T. M. SANDERS, JR.‡
School of Physics, University of Minnesota, Minneapolis, Minnesota
(Received 23 June 1966)

Electron-spin-resonance experiments on shallow donors in germanium are reported. The experiments consist of measurement of the Zeeman effect of the donors as a function of applied uniaxial compression. From the data, a value may be derived for the ratio of the valley-orbit splitting of the donor ground state ($4\Delta_c$) to the deformation potential for shear (E_2). The results for phosphorus donors agree with determinations by other workers. The result for antimony donors is $4\Delta_c/E_2=(2.08\pm0.04)\times10^{-5}$. Using the value $E_2=19.2$ eV leads to a valley-orbit splitting of $4\Delta_c=(3.99\pm0.2)\times10^{-4}$ eV. This result lies between the values obtained from piezoresistance and spectroscopic measurements. The data require that the singlet state lie below the triplet in antimony donors, just as in phosphorus and arsenic donors. An additional four-line spin-resonance spectrum in antimony-doped germanium is ascribed to donors located near the surface of the samples, in regions of high local strain.

I. INTRODUCTION

ELECTRON-spin-resonance experiments have already been shown capable of providing detailed information about the structure of shallow-donor impurities in silicon and germanium. These impurities have, furthermore, received detailed theoretical attention and present an excellent test system for the theory, since the theoretical problems are not insuperably difficult, and powerful and sensitive experiments can be brought to bear.

Since the first observation of donor spin resonances in germanium by Feher, Wilson, and Gere,[1] the spin-resonance experiments have provided values for the hyperfine splittings in phosphorus and arsenic donors, the g values of the conduction electrons, and the singlet-triplet (valley-orbit) splittings in the ground state of phosphorus and arsenic donors.[2]

The spectra of phosphorus and arsenic donors in germanium in low concentration show a resolved hyperfine structure due to the donor nucleus, and have reasonably narrow lines whose width is determined by hyperfine interactions with the Ge nuclei near the donor.

In the case of antimony-doped germanium the situation is different. The spectrum is a single, broad, and unsymmetrical line showing no resolved hyperfine structure. Perhaps for this reason there has been no attempt to use spin resonance to extract detailed information about the antimony donor.

In the experiments reported here[3] we show that application of an external stress to the sample causes a great narrowing and simplification of the line, permitting a determination of the valley-orbit splitting of the ground state. The small value of this splitting implies a very great sensitivity of the spectrum to local strain near the donor and confirms the suggested explanation of the appearance of the resonance, in a sample under no external stress, as being due to internal strain fields in the samples.

II. THEORY

A. Valley-Orbit Splitting and Effect of Strain

We will require theoretical equations relating the Zeeman effect of a shallow donor to the valley-orbit splitting and the applied stress.[4]

The theory of shallow donors in silicon and germanium has been reviewed by Kohn,[5] whose notation and approach we will follow. The conduction band of germanium has four equivalent minima (valleys) at the intersections of the [111] directions with the boundary of the Brillouin zone. Single-valley donor wave functions can be constructed from the conduction-band functions using only functions from the vicinity of the band minimum. We call such functions $\varphi_j(\mathbf{r})$, with $j=1, 2, 3, 4$ corresponding to the valleys [111], [1$\bar{1}\bar{1}$], [$\bar{1}$1$\bar{1}$], and [$\bar{1}\bar{1}$1], respectively. The functions φ_j can be written as the product of the Bloch function from the band minimum and a slowly varying envelope function satisfying a hydrogenic effective-mass wave equation. We choose the phases of the φ_j so that all $\varphi_j(0)$ are equal. In effective-mass approximation the ground state has a four-fold spatial degeneracy corresponding to the four valleys, in addition to the two-fold Kramers (spin) degeneracy. In the tetrahedral environment of a donor, removal of this spatial degeneracy can only result in the splitting of the quartet into a singlet and a triplet. The experiments to be discussed show that the singlet state lies lower than the triplet, and we shall assume this in writing the expressions which follow. The matrix representing the inter-

* This work was supported in part by the U. S. Air Force Office of Scientific Research, Research Corporation, and the U. S. Atomic Energy Commission.

† Present address: Department of Physics, Hamline University, St. Paul, Minnesota.

‡ Present address: Harrison. M. Randall Laboratory, University of Michigan, Ann Arbor, Michigan.

[1] G. Feher, D. K. Wilson, and E. A. Gere, Phys. Rev. Letters 3, 25 (1959).

[2] For a full account of the Bell Laboratories work, see D. K. Wilson, Phys. Rev. 134, A265 (1964).

[3] Preliminary results were reported by R. E. Pontinen and T. M. Sanders, Jr., Bull. Am. Phys. Soc. 6, 426 (1961).

[4] Wilson (Ref. 2) derives equivalent expressions. We present our treatment, in a form particularly convenient for our purposes.

[5] W. Kohn, in *Solid State Physics*, edited by F. Seitz and D. Turnbull (Academic Press Inc., New York, 1957), Vol. 5.

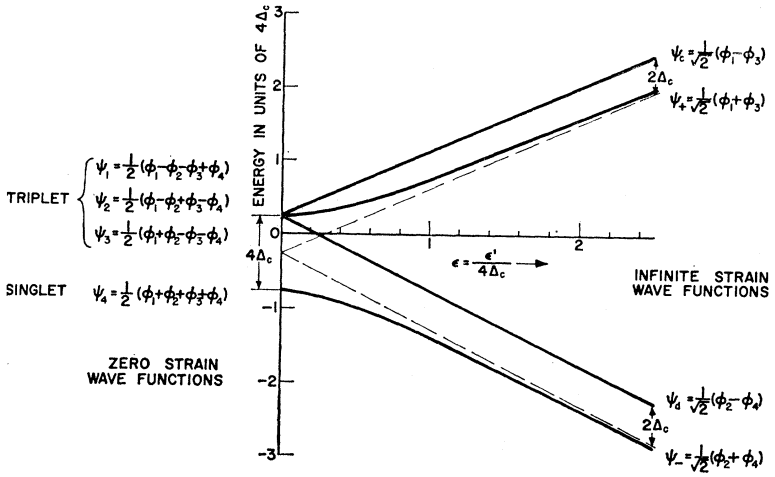

FIG. 1. Shear-induced splitting of the singlet and triplet states caused by a uniaxial compression in the [1$\bar{1}$0] direction. Wave functions for these states are given for the cases of no stress and large stress.

actions responsible for the valley-orbit splitting (or chemical shift) can be written phenomenologically in the φ representation as

$$\mathcal{H}_{c\varphi}=\Delta_c\begin{bmatrix}0&-1&-1&-1\\-1&0&-1&-1\\-1&-1&0&-1\\-1&-1&-1&0\end{bmatrix}, \tag{1}$$

which has a triplet eigenvalue at $+\Delta_c$ and a singlet at $-3\Delta_c$. Any shift of the center of gravity of the quartet is irrelevant in our work.

We now consider the effect of an applied stress on these states.[6] The present experiments used uniaxial compression in the [1$\bar{1}$0] direction exclusively. Such a stress has the effect of raising the energy of the valleys $j=1, 3$ and lowering that of valleys $j=2, 4$ by an equal amount. We write

$$\delta\epsilon_1=\delta\epsilon_3=-\delta\epsilon_2=-\delta\epsilon_4=\epsilon'=\tfrac{1}{6}E_2S_{44}X. \tag{2}$$

Here X is the force per unit area along the [1$\bar{1}$0] direction; E_2 is the deformation potential for shear; S_{44} is a shear modulus. We take X positive for compressions. The Hamiltonian matrix representing the stress is

$$\mathcal{H}_{\sigma\varphi}=\epsilon'\begin{bmatrix}1&0&0&0\\0&-1&0&0\\0&0&1&0\\0&0&0&-1\end{bmatrix}. \tag{3}$$

Thus, considering the chemical shift and the [1$\bar{1}$0] stress only, the Hamiltonian takes the form

$$\mathcal{H}_{\varphi}=\Delta_c\begin{bmatrix}\epsilon&-1&-1&-1\\-1&-\epsilon&-1&-1\\-1&-1&\epsilon&-1\\-1&-1&-1&-\epsilon\end{bmatrix}, \tag{4}$$

where we have used the notation $\epsilon\equiv\epsilon'/\Delta_c$. This matrix can be diagonalized readily. It is convenient at this point to introduce a new set of basis functions, appropriate to the special symmetry of the stress we are considering. We define the new basis functions χ_α by

$$\begin{aligned}\chi_1&=2^{-1/2}(\varphi_1+\varphi_3),\\ \chi_2&=2^{-1/2}(\varphi_2+\varphi_4),\\ \chi_3&=2^{-1/2}(\varphi_1-\varphi_3),\\ \chi_4&=2^{-1/2}(\varphi_2-\varphi_4).\end{aligned} \tag{5}$$

In the χ basis the Hamiltonian we are considering takes the form

$$\mathcal{H}_{\chi}=\Delta_c\begin{bmatrix}(\epsilon-1)&-2&0&0\\-2&(-\epsilon-1)&0&0\\0&0&(\epsilon+1)&0\\0&0&0&(-\epsilon+1)\end{bmatrix}. \tag{6}$$

It may be noted that χ_3 and χ_4 are energy eigenfunctions for all values of the strain. The energy eigenvalues are

$$\begin{aligned}w_3&=\Delta_c(1+\epsilon),\\ w_4&=\Delta_c(1-\epsilon),\\ w_\pm&=\Delta_c(-1\pm[\epsilon^2+4]^{1/2}).\end{aligned} \tag{7}$$

The energy levels and our notation are shown in Fig. 1. The eigenfunction of the lowest state can be written as

$$\psi_-=\alpha_-\chi_1+\beta_-\chi_2,$$

with

$$\alpha_-^2=2/(\epsilon^2+4+\epsilon[\epsilon^2+4]^{1/2}),\quad \alpha_-^2+\beta_-^2=1. \tag{8}$$

We choose α_- and β_- real.

B. Zeeman Effect

We have found the spatial part of the wave functions, and are now in a position to calculate the effects of spin and an applied magnetic field. Each individual valley has axial symmetry about its [111] direction. An electron in one of the states φ_j will have an axially symmetric Zeeman effect described by two parameters, $g_{\parallel}$ and $g_{\perp}$. We now calculate the Zeeman effect to be

[6] P. J. Price, Phys. Rev. **104**, 1223 (1956).

expected for an electron in a state (ψ_- of Sec. IIA) which is a linear combination of the φ_j. We use the symbols $\uparrow$ and $\downarrow$ to mean parallel and antiparallel to the applied magnetic field $\mathbf{B}_0$. Because of the tensorial nature of the magnetic moment, the component of spin parallel to $\mathbf{B}_0$ is not a constant of the motion. We write

$$\psi_{-\uparrow}=\alpha_-\chi_{1\uparrow}+\beta_-\chi_{2\uparrow}. \tag{9}$$

We will calculate the Zeeman effect to first order in B_0. Thus we need consider only the matrix elements of the Zeeman Hamiltonian connecting the states $\psi_{-\uparrow}$ and $\psi_{-\downarrow}$, which are degenerate in the absence of a magnetic field. The separation between the two spin states in the presence of the Zeeman Hamiltonian is

$$\begin{aligned}\Delta w&=2[(\psi_{-\uparrow},H_z\psi_{-\uparrow})^2+|(\psi_{-\uparrow},H_z\psi_{-\downarrow})|^2]^{1/2} \\ &=g_1\beta B_0,\end{aligned} \tag{10}$$

where g_1 is the spectroscopic splitting factor (accurate to first order) and β is the Bohr magneton. The matrix elements $(\psi_{-\uparrow},H_z\psi_{-\downarrow})$ can be written in terms of the elements $(\varphi_{i\uparrow},\mathcal{H}_z\varphi_{j\downarrow})$ by using Eqs. (5) and (8). Evaluation of the latter elements is an essentially geometrical problem, requiring specification of the direction of the magnetic field $\mathbf{B}_0$ relative to the g-tensor ellipsoids. We specify the orientation of $\mathbf{B}_0$, which is restricted to the $(1\bar{1}0)$ plane, in terms of the angle θ between $\mathbf{B}_0$ and the [001] direction. Direct evaluation of the required matrix elements and insertion into Eq. (10) leads to the result

$$g_1^2=\bar{g}^2+[\tfrac{2}{3}\bar{g}\Delta g(1-2\alpha_-^2)+\tfrac{1}{9}(\Delta g)^2(1-2\alpha_-^2)^2]\sin^2\theta. \tag{11}$$

We have made the customary[7] abbreviations,

$$\begin{aligned}\Delta g&\equiv g_\perp-g_{\parallel} \\ \bar{g}&\equiv\tfrac{1}{3}g_{\parallel}+\tfrac{2}{3}g_\perp.\end{aligned} \tag{12}$$

The result (11) takes a particularly simple form in certain special cases. Recalling from (8) that α_-^2 approaches $\frac{1}{2}$ as the strain goes to 0, and α_-^2 approaches zero for large strain, we note that $g_1=\bar{g}$ for zero strain, and

$$g_1^2=\bar{g}^2+(\tfrac{2}{3}\bar{g}\Delta g+\tfrac{1}{9}(\Delta g)^2)\sin^2\theta$$

for large strain. If $\mathbf{B}_0$ is directed in the [110] direction ($\theta=90°$), (11) becomes a perfect square, and we have the simple form

$$g_1=\bar{g}+\tfrac{1}{3}\Delta g(1-2\alpha_-^2) \quad (\text{[110] direction}). \tag{13}$$

C. Line Intensities

The donor resonance studied in these experiments is produced by donors in the lowest state (ψ_-) only, and there are low-lying excited states present (see Fig. 1). Thus the population of the significant state, and the intensity of the spin resonance, will have a temperature dependence which can provide information about the valley-orbit splitting. In the zero-strain case we may write for the population of the lowest (singlet) state,

$$n_-\propto[1+3\exp(-4\Delta_c/kT)]^{-1}, \tag{14}$$

at sufficiently low temperatures. For high strain the lowest state will mainly depopulate into the lowest excited state (χ_4) and we will have, approximately,

$$n_-\propto[1+\exp(-2\Delta_c/kT)]^{-1}. \tag{15}$$

III. EXPERIMENTAL PROCEDURES

A. Determination of Valley-Orbit Splitting ($4\Delta_c$) from g-Value Measurements

The theory developed in the last section, and Eq. (11) in particular, shows that the g value and its dependence on the orientation of $\mathbf{B}_0$ are sensitive to the form of the donor wave function. The g value is a function of the g parameters ($g_{\parallel}$ and $g_\perp$), the orientation of the magnetic field (θ), and the mixing coefficient (α_-^2) in the wave function. The last quantity, α_-^2, is in turn determined from Eq. (8) by ϵ, the ratio of the strain energy shift to the valley-orbit splitting. Determination of the valley-orbit splitting ($4\Delta_c$) is accomplished by following the variation of the donor g factor with strain. For reasons which we will now discuss, the bulk of the measurements were performed with $\mathbf{B}_0$ oriented in the [110] direction ($\theta=90°$). Among the advantages of this orientation are:

(1) The resonance width under high strain is a minimum at [110], allowing accurate g-value measurement.

(2) The g-value variation is largest at [110], with g changing from $\bar{g}$ at zero strain to $g_\perp$ at large strain.

(3) Eq. (11), relating the g value to the strain, takes on the particularly simple form (13) for this orientation.

(4) Higher order g-value corrections[8] are zero for this orientation.

A run consisted of accurate orientation of $\mathbf{B}_0$ in the [110] direction and a series of g-value determinations for various values of the applied stress.

B. Determination of the Parameters $g_{\parallel}$ and $g_\perp$

A knowledge of $g_{\parallel}$ and $g_\perp$ is required in order to extract a value of the valley-orbit splitting from the data. Only very modest accuracy is required for this purpose, however, since errors in other measurements severely limit the accuracy assigned to the value of of Δ_c. The g parameters were determined to an accuracy far greater than is required for this purpose by two independent methods:

(1) the donor g value varies from $\bar{g}=\frac{1}{3}g_{\parallel}+\frac{2}{3}g_\perp$ to $\bar{g}=g_\perp$ as the strain is varied. $\bar{g}$ and $g_\perp$ are thus directly measurable.

[7] L. M. Roth and B. Lax, Phys. Rev. Letters 3, 217 (1959).

[8] R. E. Pontinen, Ph.D. thesis, University of Minnesota, 1962 (unpublished).

TABLE I. g parameters.

	$g_\perp$	$g_\parallel$	Δg	$\bar{g}$
From new spectrum	1.9168±0.0006	0.830±0.002	1.0868±0.002 (calculated)	1.555±0.001 (calculated)
From donor g versus X^{-2}	1.9173±0.0005			
From $(g-\bar{g})^{-2}$ versus X^{-2}	1.925±0.01 (calculated)	0.842±0.01	1.083±0.01	
From P, As donors (Wilson, Ref. 2)			(As) 1.05	(P) 1.5631±0.0002 (As) 1.5700±0.0002
Observed Sb-donor resonance at zero strain				1.561

(2) The new resonance spectrum,[9] discussed in Sec. VC., follows the equation $g^2=g_\parallel^2\cos^2\varphi+g_\perp^2\sin^2\varphi$, permitting determination of $g_\parallel$ and $g_\perp$ from this spectrum.

g parameters measured by these two methods are listed in Table I. They are consistent with each other, and virtually none of the uncertainty in the final value of the valley-orbit splitting arises from this source.

C. Other Experimental Procedures

1. Orientation of the Sample in the Magnetic Field

We used light reflected from etch pits[10] to cut the sample so that the small face (see Fig. 2) was a (110) plane. The sample was positioned in the cavity so that the $(1\bar{1}0)$ plane was the plane of rotation of the magnetic field. We could check the accuracy of the orientation and locate directions in the $(1\bar{1}0)$ plane by several methods.

(a) Under no strain, the donor resonance was most easily observed when the magnetic field was in the [001] direction.

(b) The new resonance spectrum (see Sec. VC.) could be employed for an accurate orientation of the magnetic field with respect to the [001] direction. The new resonance spectrum can be described in terms of g tensors symmetrical about the four equivalent [111] directions. We could completely orient the sample by utilizing a plot of the four observed g factors as a function of the direction of the magnetic field.

(c) In the [110] direction the g factor of the donor resonance should approach $g_\perp$ as the strain becomes large.

2. Magnetic Field Determination

To determine the g factor, we must measure the microwave frequency and the magnetic field at which resonance occurs. We were interested only in relative measurements of the g factor, so that an accuracy of one part in 10^4 in determining these quantities was sufficient. The microwave frequency was compared with a frequency standard.

The strength of the magnetic field was determined with a proton resonance using a marginal oscillator detector system.[11] We modified this oscillator by the addition of a small amount of relay-switched capacitance in the tuned circuit. With this capacitance we could shift the oscillator frequency by approximately 1% so that we could calibrate the magnetic field above and below the field of the electron resonance. All measurements were made as the magnetic field was swept. Assuming that the field was swept linearly in time, we could interpolate to determine the field at which the donor resonance occurred.

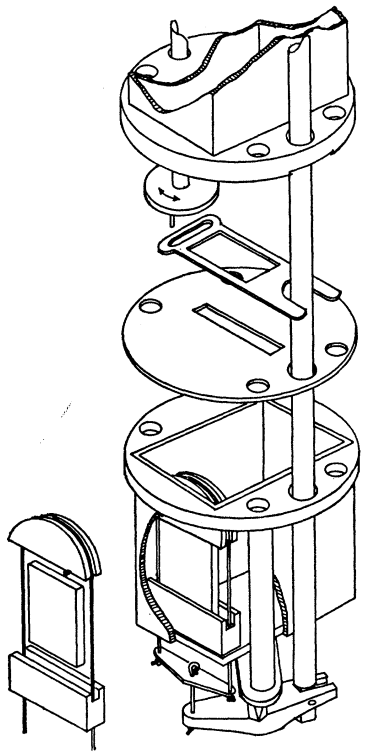

FIG. 2. Exploded view of the microwave cavity and squeeze apparatus.

[9] R. E. Pontinen and T. M. Sanders, Jr., Phys. Rev. Letters **5**, 311 (1960).

[10] G. H. Schwuttke, J. Electrochem. Soc. **106**, 315 (1959).

[11] B. Donnally and T. M. Sanders, Jr., Rev. Sci. Instr. **31**, 977 (1960).

The magnetic field was found to be uniform to within 0.3 G in the region of the electron and proton samples. No corrections were made to the measured magnetic fields, which were actually measured at the proton sample. A systematic error of approximately 0.3 G is present in our data. The determination of the magnetic field at the sample is accurate to within one part in 10^4, although relative g factors could be determined with greater accuracy.

3. *Intensity Measurements*

To determine the number of spins contributing to the donor resonance as a function of temperature, we electronically integrated the derivative of the absorption curve and then measured the area under the absorption curve with a polar planimeter. Since the Q and coupling of the cavity changed with temperature (especially above 4°K) we compared the donor absorption curve to a standard sample. The number of spins was determined for both As- and P-doped Ge. First attempts at measuring the number of spins versus temperature in unstrained Sb-doped Ge were unsuccessful because of the asymmetry and large width of the donor resonance in unstrained germanium, and also because of the low signal-to-noise ratio above 3°K. We found that when the sample was placed under large uniaxial stress the resonance became more symmetrical and its width decreased. Accurate measurements were obtained for As-doped Ge to temperatures above 10°K and for Sb-doped Ge to 6°K.

IV. APPARATUS

A. General

The spin-resonance experiments were performed using a two-bolometer bridge, x-band spectrometer.[8] We used a 6-in.-pole electromagnet, rotatable about a vertical axis. Our cryostat was a standard glass Dewar pair using liquid helium as a refrigerant and included provision for temperature stabilization in the range from 1.2 to 15°K.

B. Cavity

The rectangular microwave cavity (see Fig. 2) was operated in the TE_{011} mode and had a resonant frequency of approximately 9.5 gHz and an unloaded Q of approximately 8000 at room temperature. Coupling of the microwaves to the cavity was accomplished by placing a slotted silver plate between the waveguide and the cavity. The slot was cut (0.15 by 0.400 in.) so that the cavity would normally be overcoupled. For maximum sensitivity of the microwave bridge, it was desirable to have the cavity close to a perfect match. Because of the rapidly varying resistivity of germanium with temperature (above 4°K), the sample became a large perturbation on the cavity as the temperature was increased, and thus changed the Q and the matching. The device we used to adjust the coupling is shown in Fig. 2. A movable iris made of phosphor-bronze covered part of the slot in the silver plate. By rotating a rod extending outside the Dewar, the movable iris could be moved over the fixed slot to vary the coupling of microwaves to the cavity.

C. Squeeze Apparatus

The cavity was modified slightly so that we could apply a uniaxial compression to the sample (see Fig. 2). Two small holes were drilled through the bottom plate of the cavity (near the corners) in order to allow a 25-lb-test nylon line to pass into the cavity. The germanium sample was placed between two grooved polystyrene sample holders. The nylon line passed through the holes in the cavity, around the two holders, and was attached to a bar beneath the cavity so that the lines remained parallel. A 40-lb-test nylon line linked the bar to a short lever. The fulcrum of this lever was attached to the waveguide flange by a pair of posts. No part of the fulcrum support was in direct contact with the cavity, to reduce frequency shifts due to distortions of the cavity. The force was transmitted to the short lever by a thin-walled $\frac{1}{8}$-in.-diam brass tube with brass rods silver-soldered into each end. The upper brass rod passed through a loosely fitting O ring in the top plate and was attached to one end of a one-to-one lever outside the Dewar. We hung weights (up to 35 lb) on the lever and produced stresses up to 3×10^8 dyn/cm^2 for samples of typical cross-sectional area. We determined experimentally that the force applied to the sample was the same, to within $\frac{1}{2}$ lb, as the force applied outside the Dewar.

D. Sample Preparation

The experiments were performed on single crystals of germanium which, in most cases, were doped with antimony. The donor concentrations in the samples which we studied varied from 7×10^{14} to 7×10^{16} cm^{-3} (4.0 Ω cm to 0.04 Ω cm room-temperature resistivity).[12]

The dislocation density, as measured by an etch-pit count, was not known for all samples, but was probably less than 10^4 cm^{-2}. One crystal was grown with a low etch-pit count (2000 cm^{-2}) at one end and a high etch-pit count (12 000–20 000 cm^{-2}) at the other. We detected no difference in the donor-resonance spectra for samples with high and low etch-pit counts.

The samples were cut perpendicular to the growth axis of the crystal to minimize impurity-concentration gradients along the length of the sample. A typical sample size was $0.40\times0.24\times0.04$ in., oriented so that the smallest face was a (110) plane. The cross-sectional area of the (110) face of the different samples was varied from 0.03 to 0.09 cm^2 in order to check for systematic errors in our stress measurements.

[12] Most samples were supplied by G. Reiland of Honeywell, Inc.

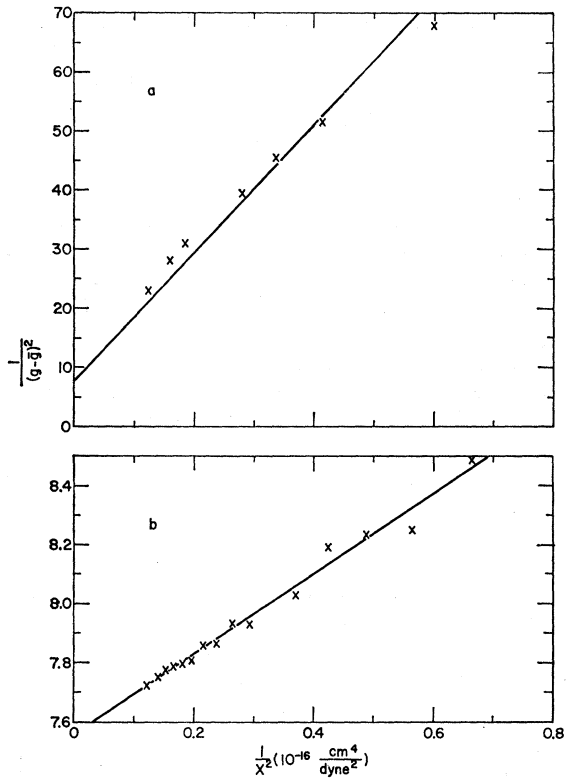

FIG. 3. Representative plots of $(g-\bar{g})^{-2}$ versus X^{-2} for two donor impurities in germanium. The magnetic field is oriented in the [110] direction. (a) 0.56 Ω cm phosphorus-doped germanium. (b) 0.15 Ω cm antimony-doped germanium.

V. EXPERIMENTAL RESULTS

A. Donor-Resonance g Values

1. Sb Donors

The donor-resonance g value was measured as a function of applied [1$\bar{1}$0] stress for a series of antimony-doped samples. The room-temperature resistivities of the samples varied from 0.15 to 3.8 Ω cm. In addition, the cross-sectional area of the samples was varied by a factor of 3 to explore the possibility of a systematic error in the value of the applied stress. A fraction of the results obtained on these samples is shown in Figs. 3 and 4. The form of the plots used in the figures was chosen as convenient in view of the result (13) of Sec. II. This result, when combined with (8), yields

$$(g-\bar{g})^{-2}=9(\Delta g)^{-2}(1+4/\epsilon^2)$$
$$=9(\Delta g)^{-2}+81(\Delta g)^{-2}(4\Delta_c)/(E_2S_{44}X^2). \quad (16)$$

Thus a plot of $(g-\bar{g})^{-2}$ versus X^{-2} should yield a straight line whose slope determines Δ_c/E_2. Figure 3 is such a plot. Curve a is for P-doped Ge, curve b for Sb-doped Ge. Equation (16) can be simplified still further in the high-strain domain ($\epsilon\gg1$). Expansion of Eq. (16) for this case yields

$$g=g_\perp-\tfrac{2}{3}(\Delta g/\epsilon^2)+\cdots$$
$$=g_\perp-\tfrac{3}{2}\Delta g(4\Delta_c/E_2S_{44})X^{-2}+\cdots. \quad (17)$$

A graph of g versus X^{-2} for high stresses should yield a straight line with intercept $g_\perp$ and slope $-\frac{3}{2}\Delta g(4\Delta_c/E_2S_{44})^2$. Figure 4 is such a plot. Only one quarter of the 240 data points taken are shown in the figure. The best values for Δ_c/E_2 were obtained from a fit to Eq. (17). The results obtained by fitting the measurements to Eqs. (16) and (17) are summarized in

TABLE II. Valley-orbit splitting.

Sample Resistivity (Ω cm)	Sample Area (cm²)	g versus X^{-2}: $g_\perp$	g versus X^{-2}: Δ_c/E_2 ($\times10^5$)	$(g-\bar{g})^{-2}$ versus X^{-2}: Δg	$(g-\bar{g})^{-2}$ versus X^{-2}: Δ_c/E_2 ($\times10^5$)
0.15	0.0581	1.9162	0.503	1.086	0.500
3.8	0.0514	1.9174	0.513	1.091	0.519
0.15	0.0918	1.9165	0.516	1.098	0.555
0.15	0.0303	1.9172	0.528	1.091	0.612
0.37	0.0525	1.9153	0.462	1.081	0.447
0.15	0.0435	1.9192	0.562	1.091	0.544
0.15	0.0435	1.9190	0.550	1.091	0.534
Average		1.9173	0.520	1.090	0.532
Least-squares fit to all data		1.9173	0.519	1.092	0.531
Probable error		0.0004	0.010	0.004	0.013

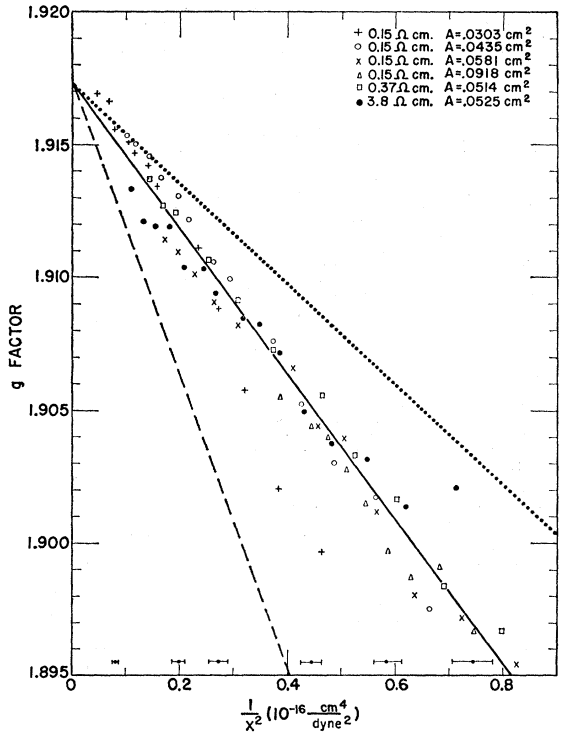

FIG. 4. The g factor of antimony donors in germanium versus X^{-2}. The external magnetic field is oriented in the [110] direction. Approximately 25% of all points used to determine $4\Delta_c/E_2$ are plotted. The error bars at the bottom indicate typical errors associated with the stress measurements. The dashed line and the dotted line correspond, respectively, to values of $4\Delta_c/E_2$ deduced from piezoresistance and infrared spectra.

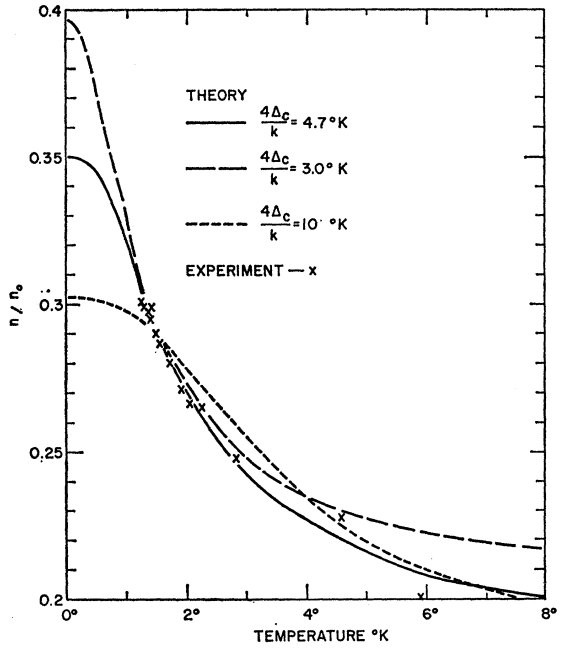

FIG. 5. Temperature dependence of the number of antimony donor electrons n and theoretical plots (Eq. 15) for various values of $4\Delta_c/k$. $X \cong 4\times10^8$ dyn cm^{-2}.

Table II. The g parameters determined from analysis of the donor spectrum are listed in Table I.

2. *P and As Donors*

As a check on the methods described here we performed measurements on P- and As-doped germanium similar to those taken on the Sb-doped samples. Some of the data on P-doped Ge are shown in Fig. 3, curve a. These data, which were not taken with great care, yield $4\Delta_c = (3.3\pm0.3)\times10^{-3}$ eV. This value seems reasonably consistent with the results of other workers.

B. Donor-Resonance Intensities

The results of intensity measurements performed on a sample are plotted in Fig. 5. Here we show the number of spins contributing to the donor resonance as a function of temperature. The data were obtained with $\mathbf{B}_0$ in the [110] direction with high stress and, as is shown in Sec. IIC, should yield some information about the value of Δ_c. However, comparison with the curves calculated from Eq. (15) for three values of Δ_c shows that the results are inconclusive. Extension of the measurements to the He^3 temperature range might permit a fair determination of Δ_c by this method.

C. New Resonance Spectrum

The four-line spectrum, whose g anisotropy is shown in Fig. 6, was studied at some length in an effort to determine the nature of the responsible spin system. Initial studies[9] established that, on one hand, the g tensors were those expected for conduction electrons, and on the other, the spectrum was almost certainly not due to electrons in the conduction band. The suggestion[13] that the spectrum might be produced by donors in sites with high local strain (e.g., donors located near dislocations) was explored by pulling a sample at a nonuniform rate. Samples were cut from opposite ends of the resulting ingot. Etch-pit counts showed less than 2×10^3 cm^{-2} for one sample and 1–2×10^4 cm^{-2} for the other. Both samples showed the new spectrum with the same intensity. At this point we concluded that the proposal of Keyes and Price was incorrect.

In the course of preparing a series of antimony-doped samples with different degrees of compensation we found, for the first time, samples in which the spectrum was not detectable. Further studies showed that the critical factor in determining the intensity of the spectrum was the surface preparation of the sample. The earlier studies used samples cut with a diamond saw and etched 6 min in a solution composed of 1 part HF, 2 parts H_2O_2, and 4 parts H_2O. Some samples were run as cut and showed virtually the same intensity of the new spectrum. Experiment showed that samples which received a heavier etch and those which were lapped and etched did not show the spectrum.

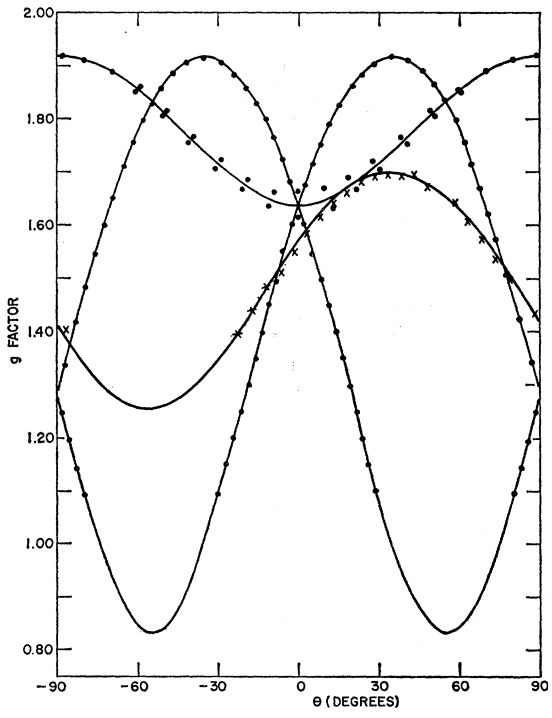

FIG. 6. The g factor of antimony donors in germanium plotted against the angle between the external magnetic field and the [001] direction. The data points indicated by x's are the "donor" resonance spectrum. The points designated by dots are the "new" spectrum. For the new resonance spectrum, the solid lines are theoretical plots using the experimentally observed values of $g_{\parallel}$ and $g_{\perp}$.

[13] R. W. Keyes and P. J. Price, Phys. Rev. Letters **5**, 473 (1960).

We conclude that the spectrum is due to antimony donors located near the surface (within 0.002 cm) in a region of high local strain. The spectrum may be of some value in studies of surface conditions in general, and surface strains in particular.

The new resonance spectrum also yielded values for the parameters $g_{\parallel}$ and $g_{\perp}$. These results are included in Table I. The values of $g_{\perp}$ determined from the new spectrum and the donor spectrum are consistent. The values for $g_{\parallel}$ are slightly inconsistent. All the results are consistent with the data of Wilson.

VI. INTERPRETATION AND CONCLUSIONS

The experiments reported here verify that in antimony donors in germanium (as in phosphorus and arsenic donors) the lowest $1s$ state is the singlet. If the triplet state were lower, the g factor of the lowest level would be strain-independent and we would not observe a single resonance at $\bar{g}$ for zero strain.

The new resonance spectrum, described earlier[9], can be attributed to electrons bound to donors near the surface, in regions of high internal strain. This confirms the suggestion of Keyes and Price.[13] g factors determined from the new resonance spectrum are quite consistent with those determined by analysis of the donor Zeeman effect under uniaxial compression.

The ratio of the valley-orbit splitting ($4\Delta_c$) to the deformation potential for shear (E_2) is determined to be $4\Delta_c/E_2=(2.08\pm0.04)\times10^{-5}$. When this result is combined with a value of E_2 (we take 19.2 ± 0.4 eV [14]), the valley-orbit splitting is determined to be $4\Delta_c=(0.399\pm0.02)\times10^{-3}$ eV. These results are in significant disagreement with independent determinations based on measurement of piezoresistance[15] and infrared spectra.[16] The discrepancy has already been discussed by Reuszer and Fisher,[16] and we have only a few comments to add to their analysis. Our measurements show that (in our samples at any rate) when no external stress is applied, the antimony donors are subject to significant perturbations. These presumably arise from internal strains, to which the antimony donor is particularly sensitive because of the very small value of $4\Delta_c$. We have not, for example, been able to understand the variation in line shape and g factor which we observe in nominally unstrained specimens.[8] On the other hand, when sufficiently large external stresses are applied, the effects of these perturbations become very small. It seems possible that the infrared spectra, which were taken without external stress, might be complicated by the effects of these perturbations. At any rate, the discrepancy between the present determination and that of Reuszer and Fisher is approximately twice the sum of the stated uncertainties of the two measurements. The discrepancy between either of these resuts and the value obtained from piezoresistance data is much larger.

ACKNOWLEDGMENTS

We wish to acknowledge the indispensable aid of R. B. Thorness and D. McIntyre in the fabrication of apparatus. During the period in which this experimental work was performed, one of us (T.M.S.) held an Alfred P. Sloan Foundation Fellowship.

[14] H. Fritzsche, Phys. Rev. **115**, 336 (1959).

[15] H. Fritzsche, Phys. Rev. **120**, 1120 (1960).

[16] J. H. Reuszer and P. Fisher, Phys. Rev. **135**, A1125 (1964).